DEFECT DETECTION AND CLASSIFICATION IN AEROSPACE MATERIALS USING PHASED ARRAY ULTRASONICS

V. Kramb[1]
[1]University of Dayton Research Institute, Dayton OH, USA

Abstract: The use of phased-array ultrasonic instruments and probes allows for optimization of both the sensitivity and resolution for detection of different defect types through electronic beam-forming, scanning, and focusing processes. However, development of these inspection processes requires an extensive database of material specimens containing known defects. Through the collaboration of the aerospace NDE community, the University of Dayton Research Institute (UDRI) has begun development of an ultrasonic database of inspection results for a variety of engine alloys and defect types. Inspections have been conducted on specimens containing a variety of synthetic and naturally occurring inclusions, voids, and defects, using the Turbine Engine Sustainment Initiative (TESI) phased array ultrasonic system. This paper will discuss current progress in the development of the ultrasonic database, and methodologies for embedded defect detection criteria.

Introduction: The use of ultrasonic inspections for the detection of hidden defects has been used extensively throughout the aerospace industry for structures, pre-production and serviced engine components, as well as material processing quality control [1,2]. This vast range of inspection applications leads to a need for inspection systems that are versatile, but can also can be customized for the detection of whatever target type is required within the parent material and component geometry of interest. The inspection applications become particularly challenging for serviced engine components. Although these components have been inspected multiple times during the pre-production stage for processing defects, the undetected defects can become altered during subsequent forming operations. Voids and inclusions, which were below the detection threshold for new components, may develop new features during service. Changes in material microstructure induced by stress and temperature result in void growth or coalescence, which could lead to crack incubation. These changes in the defect morphology may require re-inspection of the components throughout the life of the engine. The challenge to the inspection developer is to identify the pass/fail criteria for components that exhibit critical defects, while minimizing the likelihood of condemning serviceable components.

Development of a truly reliable inspection is extremely difficult in the absence of specimens that contain actual defects to be detected. In that case, inspection requirements are often developed based on practical experience with the ultrasonic response of the material and defect. This methodology for developing inspections makes use of inspector experience, which is highly subjective, and not easily quantified for the purpose of obtaining probability of detection (POD) curves. For some inspection systems, reliability is based on the probability of detecting a machined target, such as flat bottom holes (FBH) or side drilled holes (SDH) of various sizes. Correlations between the response from machined targets upon which the POD curves are based, and the natural targets to be detected are often limited however, and thus the probability of detecting the natural targets is largely unknown. Significant improvements in the reliability of the POD curves would be expected if synthetically produced targets, which represent the type and range of reflectivities expected from the natural defects were used. Specimens produced with targets that are more representative of the actual inspection condition could then be used to generate POD curves that are directly related to the probability of detecting the defects of interest.

Specimens that contain synthetically produced natural targets over a range of reflectivities, can also be used to develop defect detection criteria. Analysis of the A-scan waveforms may provide information about the target that can be used to identify the defect type. Previously, collecting A-scans during an inspection was impractical due to the memory required for data storage. Current technology however, permits the acquisition and storage of large quantities of A-scan data, thus permitting a new approach to defect detection and classification.

Current inspection procedures make use of C-scan amplitude data only to make pass/fail decisions. These decisions are derived using various algorithms based on a calculated amplitude within the suspect region, which is compared to a calculated amplitude of the surrounding material background noise level. These algorithms are very carefully controlled and monitored since they are what ultimately decide the risk level of the inspection. Since aerospace components can contain a variety of defects however, it would be beneficial to determine not just the relative "size" of the target, or it's severity based on a signal to noise ratio, but the actual type of defect that has been located based on some feature or property of the A-scan.

Under the Turbine Engine Sustainment Initiative (TESI) a new approach for determining POD and defect detection is currently being developed. Specimens are being produced that will contain selected targets representing the range of reflectivities expected for embedded defects in turbine engine components. These targets currently include carbon, alumina and tungsten, with calculated reflectivities of 0.8, 0.34 and 0.08 respectively, in Rene [3]. These specimens (Number 1 and 4 in Table 1) were produced with a titanium or Rene matrix material, which was ultrasonically clean with very little background material noise. The embedded defect targets examined in the current study are 3mm spheres. Good mechanical bonding between the target and matrix material was insured through ultrasonic and metallographic examination. In addition to the spherical targets, 2 target locations were prepared but did not contain spherical targets during final specimen processing. These locations remained as a discontinuity in the matrix material after processing; however the exact morphology of the remaining void is unknown. The simulated void targets are included with the spherical targets in the specimen description as an example of an irregular void type defect.

Based on the ultrasonic response from these targets, advanced methods for defect classification, based on A-scan correlation and classification methods, will be explored. In addition, the ultrasonic response from these new specimens will be compared to the ultrasonic response from traditional machined and synthetically produced targets. Through the cooperation of the NDE aerospace community, many specimens have been made available to the TESI program for this comparative study. During the study, inspections will be conducted on all available embedded defect specimens, and the data compiled to create an ultrasonic database. The database will include data from a wide variety of targets, transducers and inspection conditions, which will be made available to the aerospace NDE community. Ultimately, this database could be used to assess the detection capability of new systems and techniques as they become available. A summary of the embedded defect specimens that have been made available to the TESI program thus far is shown in Table 1. Inspections on these specimens are currently in progress, and will continue as new specimens and inspection techniques become available. The discussion in this paper will focus on the ultrasonic response from targets roughly 12mm deep, within a nickelbase superalloy matrix. (Specimens #4-8 in Table 1).

Results: The experimental setup used in this study consists of the R/D Tech Tomoscan III pulser/receiver, gantry x-y scanning system, conventional single element and multi-element linear array transducers. The data presented in this paper were acquired using 10MHz, 3" focus, 0.375" diameter single element transducer, (UTX, Inc. 112 Milltown Road, Holmes, New York) and a 10MHz, 64 element, (0.45 X 5.0mm element size) linear array transducer (R/D Tech Ultrasound Transducers, 60 Decibel Rd., State College PA). Although linear array transducers have been widely used in applications such as pipeline, power generation and weld inspections [4,5], the use of phased arrays in aerospace ultrasonic inspections is not as common. Therefore, it is of value to compare inspection results obtained using both conventional and linear array transducers on aerospace relevant materials and targets. This paper will discuss the results obtained thus far in the development of inspection processes for turbine engine components using phased array transducers. A more detailed comparison of the ultrasonic response from phased array and conventional transducers is discussed elsewhere in these proceedings.

Table 1.
Embedded defect targets examined under the TESI program (current status).

Specimen number	Matrix material	Target	Target Depth (mm)	Size (diameter)
1.	Titanium	W	12.7	3mm
		C	12.7	3mm
		Al_2O_3	12.7	3mm
		void	12.7	irregular
2.	Titanium	SHA* (1.6, 2.7, 5.9%N)	25.4	#2-5 FBH
3.	Titanium	FBH	3.175-76.4	#1-5
4.	Rene95	W	12.7	3mm
		C	12.7	3mm
		Al_2O_3	12.7	3mm
		void	12.7	irregular
5.	Rene95	SDH	3.175-76.4	0.020 in.
6.	IN100	FBH	1.5-76.4	#1/2-3FBH
7.	PM IN100	SiO_2	10.0	0.177-0.250mm
8.	PM IN100	Al_2O_3	12.0	0.149-0.297mm
9.	IN100	mal-oriented, penny shaped defects	3.8-42.5	#1-5FBH
10.	Aluminum	SDH	1.5-70.2	0.4-1.6mm
11.	Aluminum	FBH	12.7	0.4-1.6mm

*Synthetic Hard Alpha inclusions (SHA)

All inspections in the current study used a mechanical scan and index resolution of 0.5mm. For the linear array transducer, electronic scanning in the index direction was combined with mechanical stepping when needed to acquire data over the entire inspection volume. This work attempted to use each transducer as they are typically used for normal incidence inspections. Single element transducers have a fixed focal length, and are usually focused on the surface of the test object. For subsurface inspections with fixed focus transducers a depth-amplitude correction (DAC) is typically applied to achieve the required sensitivity deeper in the part. The phased array transducer on the other hand, can be focused at whatever depth provides the optimum sensitivity for the particular inspection. Depth amplitude corrections for the array transducer can then be constructed in the instrumentation as needed. In the current study, the linear the array transducer was positioned for a 25 mm water path, and the normal incidence beam was focused inside the part near the plane of the target.

Prior to each inspection, the transducer response was calibrated to an 80% full scale height (FSH) peak amplitude from a #1FBH located 0.5" deep in titanium (Ti-6V-4Al). The RF A-scan and rectified peak amplitude C-scan from each of the embedded defect specimens was then recorded. Targets which produced a reflection exceeding 100% peak amplitude based on a #1FBH calibration were rescanned with a lower gain setting in order to obtain the frequency content of the reflection. In the following figures, the A-scans are displayed as the full waveform data, while the C-scan data has been rectified to improve the image contrast. Further details of the inspection system and calibration approach can be found in [6].

Discussion: C-scan and typical A-scan response from the spherical targets in Rene (specimen 4, Table 1) are shown in Figure 1 above. The C-scans show that both transducers were able to detect the high reflectivity targets, carbon and tungsten, very clearly. The alumina target is barely detectable with the linear array transducer, and not visible above the matrix material noise with the single element transducer. A comparison of the C-scan and A-scan data from the two transducers also shows that the peak background noise level away from the defect was slightly higher for the single element transducer than the array transducer, 5% and 2% respectively. The increased noise was due in part to the higher gain (≈+6db) required to calibrate the conventional transducer to #1FBH sensitivity. The amplitude data from each of the targets is summarized for the two transducers in Table 2.

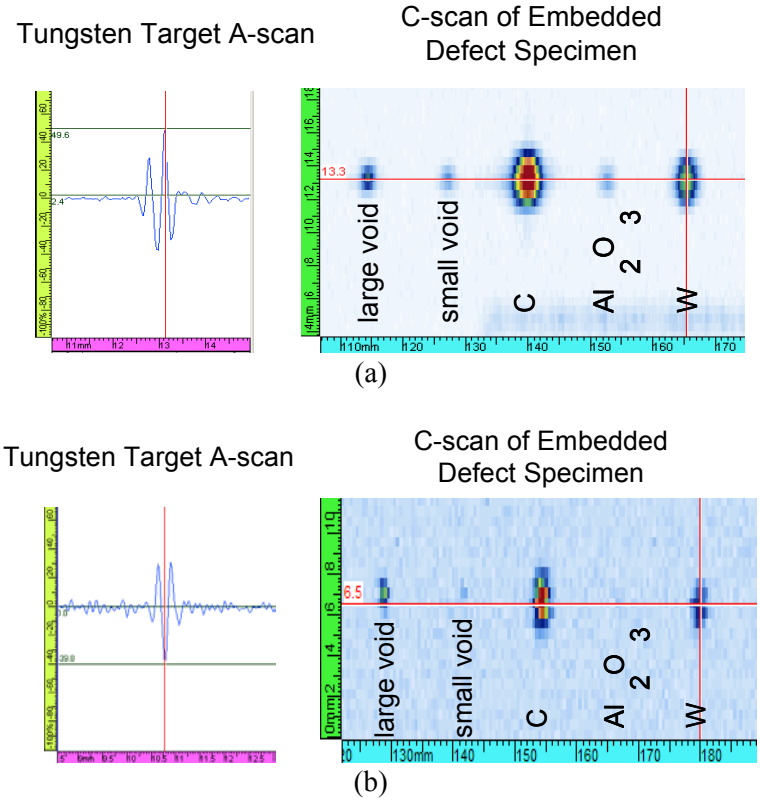

Figure 1: Representative A-scans and C-scans of embedded defect specimen. obtained using a (a) 10 MHz, 64 element linear array, 16 element focal law, focused at 0.5 inches below the surface, 25 mm water path (b) 10 MHz single element, 3" focused transducer, 3" water path.

Frequency content of the peak A-scan was also examined. The peak frequency and –6dB bandwidth were recorded for each target reflection, and the results summarized in Table 2. Although the data indicate that there may be a correlation between the frequency response from spherical targets and the irregular voids, further studies are required on many more specimens to determine the relationship.

Table 2.
Embedded defect ultrasonic response, Rene matrix.

			Linear Array			Conventional Single Element		
reflector	long. velocity	calculated reflection coefficient	peak amplitude	peak frequency	-6dB bandwidth	peak amplitude	peak frequency	-6dB bandwidth
	(mm/μs)		(% FSH)	(MHz)	(%)	(% FSH)	(MHz)	(%)
carbon	3.018	0.81	100	8.4	67	100	11.3	71
alumina	10.598	0.09	14	8.8	15	3	12.5	14
tungsten	5.212	0.34	50	8.2	64	40	11.7	60
sm. void			16	7.4	50	14	8.5	62
lg. void			39	11.1	51	48	12	34

Inspections conducted on the PM IN 100 specimens (#7, 8, Table 1) also show the effect of varying defect size and reflectivity on detection sensitivity. Figure 2 shows C-scans obtained using the 10 MHz linear array transducer to inspect SiO_2 and Al_2O_3 irregularly shaped targets approximately 0.250 mm in diameter. For both scans, the transducer was focused at 5 mm, and the gain adjusted to achieve an 80% FSH peak height from a #1FBH at the same depth as the embedded defects (0.25 in.). Although the particles are roughly the same size between the two specimens, the increased reflectivity of the silica (≈0.58) over the alumina (≈0.08) results in a significantly higher reflection amplitude. The reflected amplitude from the 0.250 mm diameter Al_2O_3 particles defects can also be compared to the reflections from the 3 mm diameter alumina spheres discussed above. Figure 1 showed that a 10X increase in particle diameter produced a detectable reflection for the alumina with the linear array transducer. These results indicate that for detection of low reflectivity targets, such as alumina defects smaller than 3 mm, further development of the inspection approach is required. For higher reflectivity targets, such as SiO_2, tungsten and carbon, the 10MHz linear array with normal incident beams appears to be adequate for defects larger than 0.250 mm in diameter.

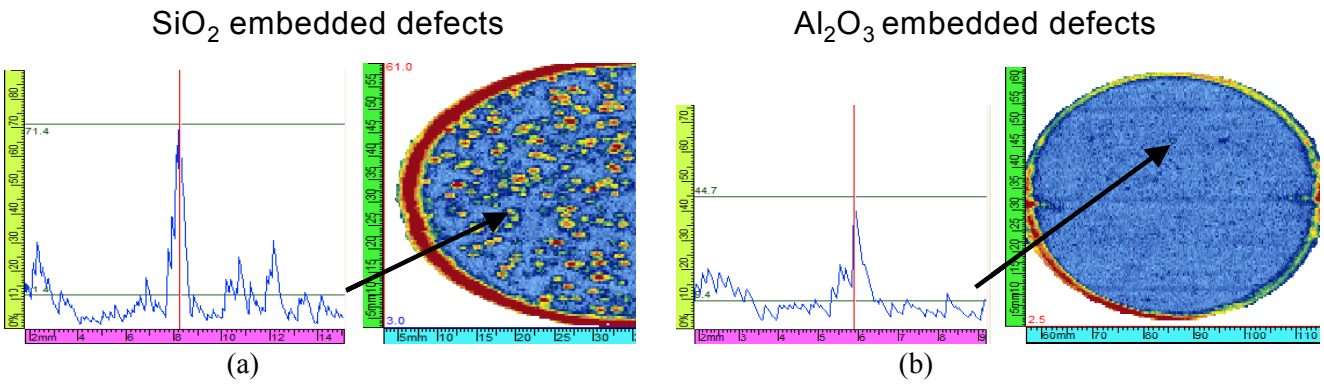

Figure 2: Representative A-scans and C-scans of PM IN100 embedded defect specimens acquired using a 10MHz, 64 element linear array, 16 element focal law, focused at 5 mm (a) SiO_2 irregularly shaped targets 0.177-0.250 mm in diameter (b) Al_2O_3 irregularly shaped targets, 0.250-0.297 mm in diameter.

The results presented thus far on simulated defects show that the expected response from conventional and array transducers is similar over this range of embedded defect size and reflectivities. One limitation of the embedded defect specimens however, is that the targets are located at a fixed depth from the surface of the specimen. In an actual inspection, defects are distributed over a range of depths, where the effects of attenuation and non-uniform beam properties can affect the inspection sensitivity. In order to determine the optimum inspection conditions, the ultrasonic beam profile must be characterized over a range of depths. Under the TESI program, probe characterization blocks have been designed and produced, which contain closely spaced SDH and FBH targets from 0.125-3.0 in. depth. These blocks have been used to characterize the beam profile over the entire depth of the block. It is hoped that by correlating the ultrasonic response of the simulated defect at a particular depth with that of a of machined target that is characterized over many depths, the sensitivity to natural targets over the entire inspection depth can be derived. In the discussion below, the initial characterization of a single SDH and FBH reflector located at the same depth as the simulated targets, ≈12.7 mm, will be examined. The results of a study conducted to characterize the ultrasonic beam profile from a depth of 3-76 mm is discussed in further detail elsewhere in these proceedings.

The linear array transducer was scanned across the SDH block using 3 beam focusing conditions: 3mm, 19 mm and 35 mm. The A-scans shown in Figure 3(a) show that the peak reflected amplitude is directly related to the focal law used in the inspection. The results show that the highest amplitude was obtained when focusing near the target plane. Thus, focusing at 19 mm produces the highest amplitude reflection from the 12.7mm deep hole, while focusing far above or below the SDH target produces a lower amplitude reflection. This result is not surprising and simply illustrates the effect of beam focusing. However, these are inherent differences between the beam profile generated by the array transducer and that of a single element transducer focused at the part surface. The A-scan for the single element transducer is shown in Figure 3(b). Single element transducers focused at the surface of the part are expected to show a continuous decrease in amplitude with depth, which is commonly compensated for with a depth (or time) compensated gain correction. The differences in beam profile between array transducers and conventional transducers as a function of depth, indicates that development of an inspection procedure should also require beam profile characterization studies. Characterization of the beam profile can then be used to develop focal law dependent depth corrections, which insure that the required sensitivity is achieved over the entire depth of interest for all focal laws used.

The frequency content of the side drilled hole reflections is summarized in Table 3. As was observed for the spherical targets, the peak frequency for the array transducer was shifted to 8.8 MHz from the nominal 9.9 MHz. The single element transducer did not exhibit a frequency shift for the reflection from side drilled holes.

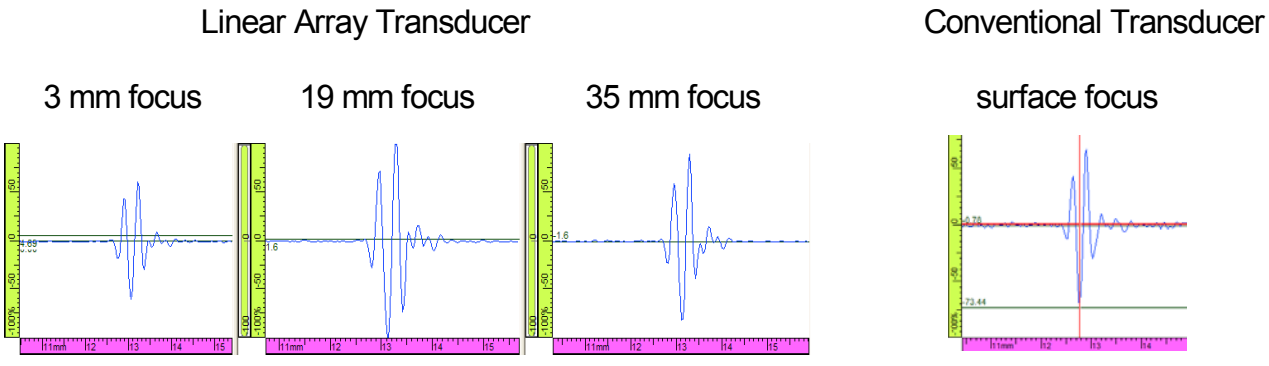

(a) (b)

Figure 3: Representative A-scans from side drilled hole 12.6 mm deep in Rene 95. A-scans were acquired using a (a) 10MHz, 64 element linear array, 25 mm water path and (b) 10 MHz single element, 3" focused transducer, 3" water path.

Table 3.
Side drilled hole ultrasonic response, Rene matrix.

Linear Array				Conventional Single Element		
focal depth	peak amplitude	peak frequency	-6dB bandwidth	peak amplitude	peak frequency	-6dB bandwidth
(mm)	(% FSH)	(MHz)	(%)	(% FSH)	(MHz)	(%)
3	57	8.6	67	73	10	60
19	100	8.8	68			
35	98	8.8	63			

The ultrasonic response from machined flat bottom hole targets can also be used to characterize the beam profile inside a component or part. Figure 4 shows results obtained using the 10MHz linear array, focused at 10mm depth, to inspect an IN100 specimen containing FBH targets (specimen #6, Table 1). Transducer calibration for this inspection was performed by adjusting the transducer gain to achieve an 80% FSH reflection from a #1FBH 11 mm deep. The FBH reflection shown in Figure 4(a) is typical for this specimen. The FBH targets were drilled very close to the bottom of the specimen, and therefore it was difficult to obtain a full waveform without interference from the back surface reflection. Nevertheless, a peak frequency of 8.8 MHz and –6 dB bandwidth of 67% was calculated for the A-scan in Figure 4(a). These values are in agreement with the results obtained on other reflectors discussed above. The table in Figure 4(b) summarizes the peak amplitude data obtained on several FBH targets located at a depth of 11 mm. The peak amplitude data shown below indicates that the linear array transducer has sufficient sensitivity to detect machined defects of comparable size, at the same depth. Thus, specimens containing #1 FBHs over the depth range of interest, would be instrumental for characterizing the focused beam profile for the development of the optimum inspection conditions.

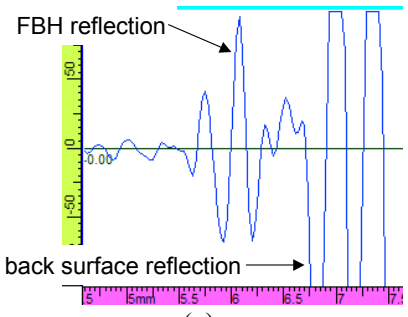

(a)

10 MHz Linear Array FBH sensitivity

Specified FBH diameter	depth	amplitude	Signal/Noise
(in)	(in)	(%)	
0.008	0.427	22	13.8
0.014	0.427	63	54.2
0.016	0.427	81	40.5

(b)

Figure 4: UT response from FBH reflectors in IN100 using 10 MHz linear array transducer: (a) Peak A-scans from #1FBH hole 6 mm deep in Rene 95. (b) FBH sensitivity at a depth of 0.427 in.

Conclusions: Under the Turbine Engine Sustainment Initiative (TESI) a new approach for determining embedded defect sensitivity and detection criteria is currently being developed. Results obtained thus far indicate that specimens containing targets, which represent the range of reflectivities expected for embedded defects, can be used to simulate natural defects for inspection development. Correlations between the ultrasonic response from these simulated defects and machined targets such as FBHs and SDHs can be used to determine the expected sensitivity as a function of depth in the part. A-scan and C-scan data obtained using linear array transducers were compared to that from single element focused conventional transducers. Similar sensitivities for both the conventional and linear array transducers showed that both transducers are applicable for inspections over the range of depths and target reflectivies discussed. Further studies are under way to fully characterize the focused beam profile inside the component, and to examine the response of the array transducers to targets with different reflectivities within other matrix materials, using angle beams as well as normal incidence.

Acknowledgements: The author would like to thank the following people and organizations who graciously loaned their specimens to the TESI program: Iowa State University, Ames IA; Pratt and Whitney, Columbus GA, MTU Aero Engines, München Germany. All spherical target embedded defect specimens were developed and produced, under contract, at the General Electric Aircraft Engines Corporate Research Center, Schenectady NY. All work was sponsored by the Turbine Engine Sustainment Initiative, administered by the United States Air Force under contract# F42620-00-D-0039,RZ02. In addition, the author would like to thank the numerous members of the University of Dayton Research Institute who have contributed to the success of this project.

References:

1. B.Lacroix, V. Lupien,, T. Duffy, Kinney, A., P. Khandelwal, H. S. Wasan, in *Review of. Progress in .QNDE.* Vol. 21**,** op. cit., (2002), p. 861.

~~[7]~~2. J. Selman, J. T. Miller, M. D. Moles, O. Dupuis, and P. G. Herzog, ., in *Review of. Progress in .QNDE.* Vol. 21**,** op. cit., (2002), p. 886.

3. J. Bartos, *Proceedings of the First Workshop on Phased Array Ultrasonics*, University of Dayton, Dayton OH, March 2004.

4. M. Moles, in *Review of. Progress in .QNDE.* Vol. 21**,** eds. D. O. Thompson, D. E. Chimenti, Plenum, New York, (2002), p. 902.

5. A. Lamarre, N. Dube, P.Ciorau, B. Bevins, NDTnet, Vol. 2, No. 12, (1997).

6. V. A. Kramb, R. B. Olding, J. R. Sebastian, W. C. Hoppe, D. L. Petricola, J. D. Hoeffel, D. A. Gasper and D. A. Stubbs, in *Review of. Progress in .QNDE.* Vol. 23**,** eds. D. O. Thompson, D. E. Chimenti, Plenum, New York, (2004), p. 817